

RESEARCH

Open Access



A ball-jointed tendon-driven continuum robot with multi-directional operability for grasping objects

Ryo Onose^{1*} and Hideyuki Sawada²

Abstract

A continuum robot, inspired by biological features, flexibly bends its body and conforms to various shapes. The high compliance and low stiffness, however, causes low rigidity and ambiguity in control when it is applied to grasping and manipulating an object. In this study, we develop a ball-jointed tendon-driven continuum robot that can bend to arbitrary directions for manipulating and grasping an object. Discs are connected by ball joints, together with coil springs coupled with tendon threads, and form a backbone of the robotic body. The continuum robot is operated to bend to an arbitrary direction by pulling the tendons using three servomotors, and returns to the original straight shape by releasing the pulling force of the contracted coil springs. The robot is constructed by using 3D-printed parts. In the experiment, the ability of the multi-directional operation was tested by bending the continuum body to specific directions, and then performing arc-following motion. Furthermore, the manipulator's grasping performance was demonstrated by preparing five objects that have various shapes, sizes, and softness. The robot successfully grasped all the objects by wrapping around them and adapting its shape to the object's shapes. The experiments verified the satisfactory operability of the continuum robot.

Keywords Continuum robot, Tendon driven robot, Grasping manipulation

Introduction

Conventional robots with rigid links and joints are typically used in industry, and they can move quickly and accurately [1]. However, these rigid structures can be dangerous in human-interactive environments. Unlike these robots, continuum robots are usually made entirely of soft materials and are mainly inspired by biological features such as an elephant trunk [2–4] and an octopus [5], and they can bend (and sometimes stretch and twist) at any point along the body structure [6]. Thus, the high compliance of a continuum robot can improve the safety

concerns. Also, since continuum robots can be actuated to conform to various shapes, robots are used for multiple tasks, such as rescuing in collapsed buildings [7] and minimally invasive surgery [8, 9].

Various actuating methods for continuum robots have been developed, including pneumatic actuation [10, 11] and actuation by shape memory effect [12]. One of the most common actuation methods is to use tendon structure, in which several tendons are routed along the flexible backbone of the robot, and the bending motion is achieved by pulling the tendons [13–15]. Compared to other actuations, tendon actuation is more compact in size and capable of large motion.

One of the advantages of continuum robots is the ability to grasp objects with the entire arm, called “whole arm grasping” [16]. The conventional manipulators which operate objects by its end effector can operate only relatively light objects. On the other hand, the whole arm

*Correspondence:

Ryo Onose
onoseryo@uri.waseda.jp

¹ Department of Pure and Applied Physics, Graduate School of Advanced Science and Engineering, Waseda University, Tokyo, Japan

² Faculty of Science and Engineering, Waseda University, Tokyo, Japan

grasping distributes the contact points between the robot and the object, thus it reduces the actuation power and improves the ability to manipulate heavy objects [17]. Furthermore, since there is no restriction by the end effector, objects of various sizes can be grasped [16].

In the effective use of soft continuum robots for grasping an object, their high compliance and relatively low structural stiffness may cause a problem: soft materials have limited stiffness, and small interaction forces generate the significant deformation of the robot itself [18]. To control the stiffness of a robotic body is one solution to solve this problem. Jamming, which is a pressure-induced control method, is widely studied [19, 20], and several continuum robots that use jamming successfully grasp objects [21, 22]. However, jamming gripper robots are constructed by a complex structure, and require an air pump to trigger jamming.

The combination of a soft body and the rigidity can be another solution to tackle this problem. Several robots driven by the tendon have been proposed [18, 23]. Although these robots successfully grasp objects having various shapes and sizes, the direction of motion is limited, and the free motion like actual living creatures has not been achieved.

By considering a flexible joint with high rigidity having no restrictions on the direction of motion, we introduce a ball joint that has been used in tendon-driven robots [18, 24–27]. Compared to other flexible joints that allow movement in arbitrary directions such as gimbals, ball joints are easier to fabricate and less expensive. In this study, by using balls for joints, we develop a tendon-driven continuum robot manipulator with simple structure that can achieve flexible movement to bend arbitrary directions for grasping objects by wrapping around. The operability and the grasping performance of the robot are experimentally verified.

Methods

Robot design

The schematic structure and the operation of the tendon-driven continuum robot constructed in this study are illustrated in Fig. 1. In order to achieve flexible motion in all directions and to have the rigidity required to grasp different objects, we employ balls for the connection between the discs. Eight discs and seven balls are connected to each other, and an operon rubber string is threaded inside the balls to connect them. The discs are also connected to each other by compressed coil springs, and threads are penetrated inside the springs to work as tendons.

From the initial state (Fig. 1a), by pulling the threads toward the base using servo motors, the robot bends its body (Fig. 1b). Then, by releasing the pulling force,

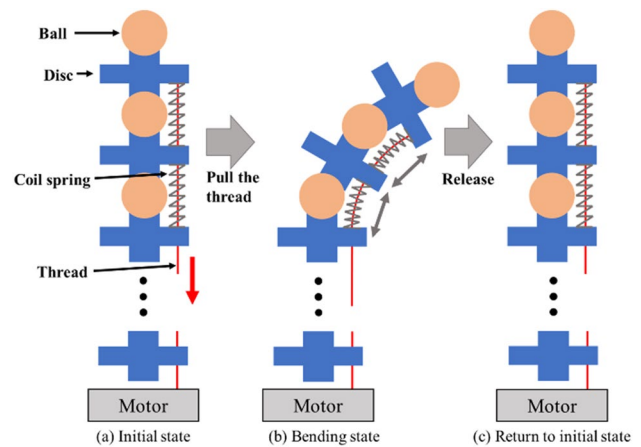


Fig. 1 Structure and operation of the robot

the restoring force of the contracted springs returns the manipulator to its initial state (Fig. 1c).

In consideration of the dimensions of the parts, the shape of the bent manipulator is illustrated by Fig. 2: if the maximum angle at which one joint can bend is 2θ , the diameter of the hole in the disc ϕ can be expressed as

$$\phi = 2r_{ball} \sin \theta \tag{1}$$

where r_{ball} is the radius of the ball.

Assuming that each point in the entire manipulator bends at an equal angle, the entire manipulator takes the form of an arc, as shown in Fig. 2c. Then, the distance between balls d can be expressed as

$$d = 2R \sin \theta \tag{2}$$

where R is the radius of the arc.

When $\phi=15$ mm, $r_{ball}=10$ mm, and $d = 35$ mm, the radius of the arc formed by the manipulator is calculated as $R = 23.33$ mm, which means that the radius of the disc should be about 20 mm to be able to wrap around a small object.

Robot fabrication

The dimensions of the parts are determined to satisfy the above requirements, and the disc is designed as shown in Fig. 3. The large hole in the disc center shown in Fig. 3a is fabricated so that the rubber string is threaded inside the balls to connect the robotic body from the base to the tip. Three holes for tendons are settled at every 120 degrees so that the bending angles in arbitrary directions are controlled by pulling tendons from three directions.

A 3D printer (CR-10 Smart, CREALITY) is used to fabricate the discs using the PLA (Polylactic acid) material. The wooden-made balls with the diameter of 20 mm are employed. The properties of the coil spring are shown

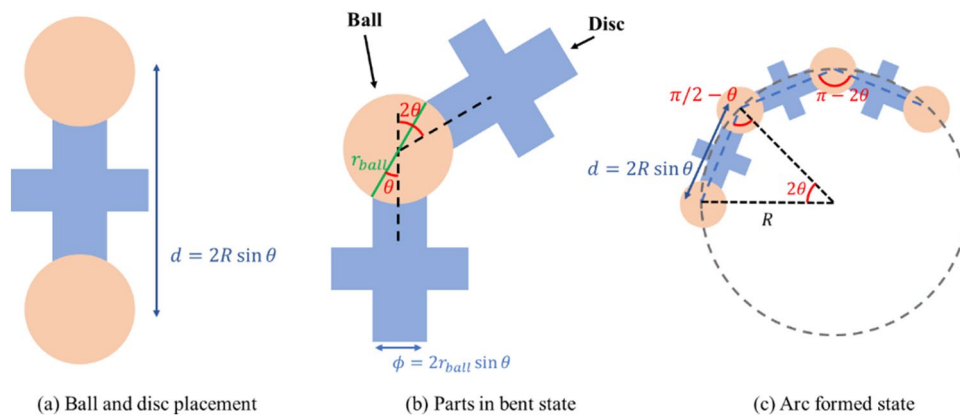


Fig. 2 Shape of the bent manipulator

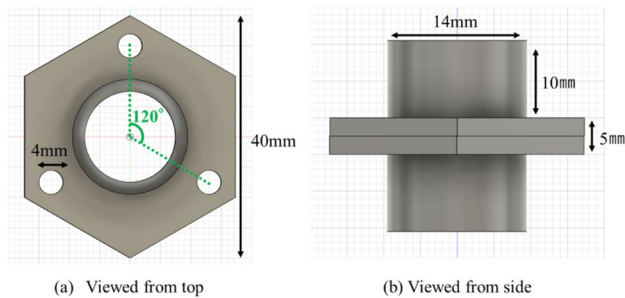


Fig. 3 Design of the disc

Table 1 Properties of springs

Material	Height (mm)	Diameter (ϕ)	Spring constant (N/mm)
SUS304WPB	30	5	0.078

in Table 1. The appearance of the completed manipulator is shown in Fig. 4. The total length and weight of the manipulator were 270 mm and 80 g, respectively.

Next, the force required to wind the manipulator was measured in order to select motors to pull the tendons. Using a spring scale, the force required to wind the manipulator was determined to be approximately 0.52 kgf. We set the radius of the spindle, which is attached to the motor axis where the tendons are wrapped, is set at 5 cm, so the required torque is $0.52 \times 0.5 = 0.26$ [kg · cm]. A 360° continuous rotation servo motor SG90-HV is employed, and the characteristics of this motor are shown in Table 2.

Referring to the dimensions of the motors, we design a stand to fix three motors, and fabricate it using the 3D printer. Each motor is controlled by Arduino UNO. The overall appearance of the robot is shown in Fig. 5.

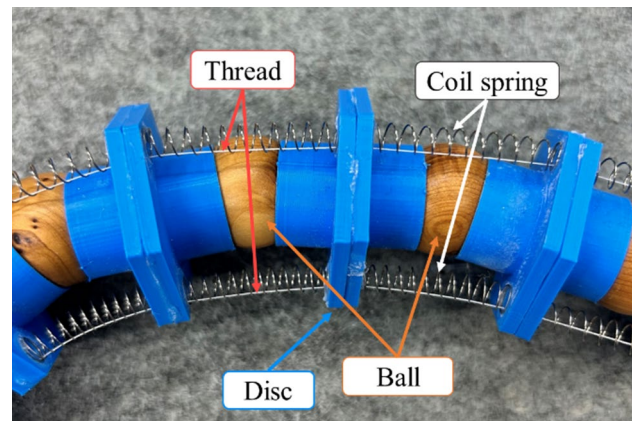


Fig. 4 Structure of the manipulator

Table 2 Characteristics of the motor, SG90-HV

Weight (g)	Dimension (mm)	Stall torque (kg · cm)
9	23 × 12.5 × 22	1.3 (4.8V), 1.5 (6V)

To verify the performance of the robotic behavior designed as shown in Fig. 1, we firstly tested the bending motion by manipulating one thread. An example of the motion result is shown in Fig. 6, where the numbers in Fig. 6a show the time in second taken from the initial state, and then back to the initial position. Figure 6b presents the trajectory of the tip position at each time, in which the 5 locations presented in the pictures from (A) to (E) are also indicated. We confirmed that by pulling the thread, the robot was bent successfully to the direction where the thread was settled. By releasing the thread, the robot instantly returned to its original straight shape.

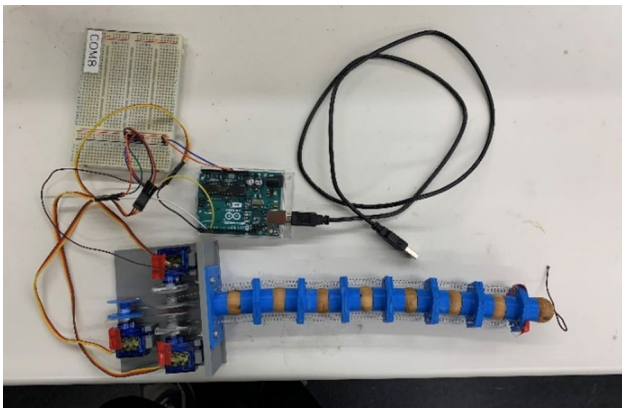


Fig. 5 Appearance of the robot

Control program

The bending operations are executed by changing the length of tendons driven by the servo motors. The control program needs to calculate the amount of rotation of each motor according to the direction of bending. Assuming that the curvature of the manipulator is constant, the model of bent manipulator is defined as shown in Fig. 7.

We also assume that the backbone is constant with the length L_0 , and the length of a tendon L can be expressed as follows:

$$L_0 = \alpha r_0 \tag{3}$$

$$L = \alpha(r_0 + \Delta r) \tag{4}$$

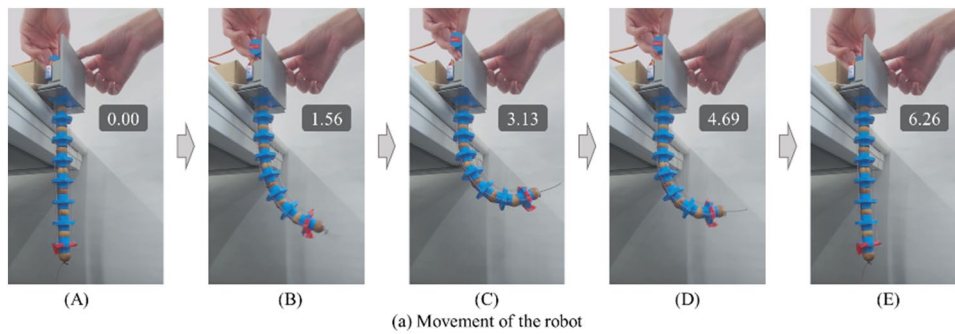
where the radius of the arc is r_0 , the center angle of the arc is α , and the distance between the tendon and the backbone is Δr .

Therefore, the increase in the length of the tendon ΔL is then

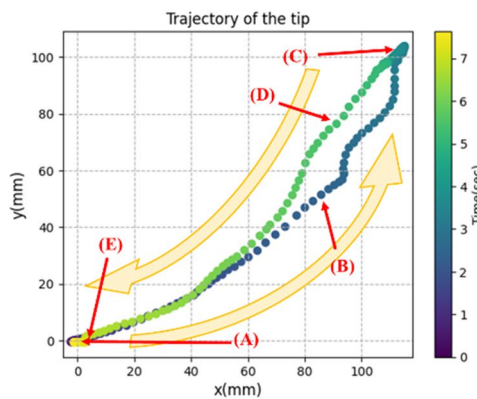
$$\Delta L = L - L_0 \tag{5}$$

$$= \alpha \Delta r \tag{6}$$

Next, by ignoring the diameter of the hole through which the tendon passes, a model of the positions of the tendons is defined as shown in Fig. 8. Three tendons in Fig. 8 are named Tendon 1, Tendon 2, and Tendon 3, respectively. We denote Δr for each tendon as Δr_1 , Δr_2 , and Δr_3 , which can be calculated by the following equation:



(a) Movement of the robot



(b) Scatter plot of the tip position

Fig. 6 Operation test of the robot

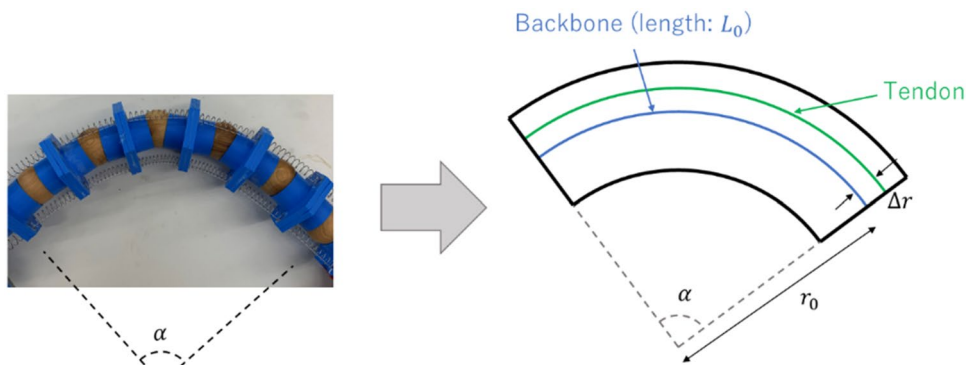


Fig. 7 Model of bent manipulator

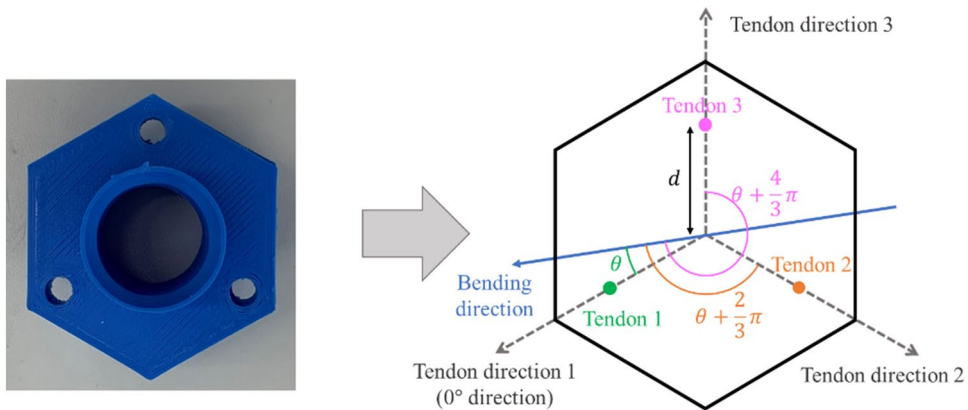


Fig. 8 Three positions of tendons and 3 principal bending directions

$$\Delta \mathbf{r} = \begin{pmatrix} \Delta r_1 \\ \Delta r_2 \\ \Delta r_3 \end{pmatrix} = -d \begin{pmatrix} \cos \theta \\ \cos \left(\theta + \frac{2}{3}\pi \right) \\ \cos \left(\theta + \frac{4}{3}\pi \right) \end{pmatrix} \quad (7)$$

where d is the distance between the backbone and a tendon, θ is the angle between the direction of motion and the direction of tendon 1.

From the Eqs. (6) and (7), we obtain the relationship between the direction of bending and the amount of change in tendon length. Based on the calculations, the robot can bend to a specific direction by pulling the threads to the required lengths.

Experiment and results

Multi-directional operation

The operability to bend to arbitrary directions was examined. We conducted experiments in which our manipulator was operated in various directions.

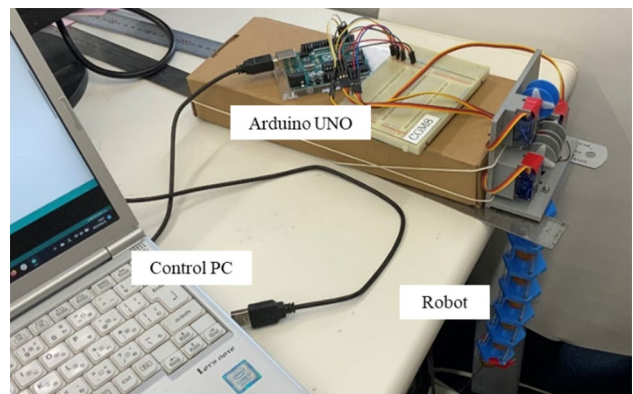


Fig. 9 Experimental environment

The base of the robot was fixed at the edge of a table as shown in Fig. 9, and the continuum robot was suspended from the base. In this experiment, the bending direction 0° was set to the direction of the tendon 1 as shown in

Fig. 8, and the bending angle was defined in the clockwise rotating direction. The bending manipulation is conducted by giving 3 control values to the tendon-driving motors as $m(T_1, T_2, T_3)$. For example, to bend the robot to the 60° direction, the control value $m(5, -10, 5)$ is given to the motors. The robot was operated to bend to five different directions, which were observed from the floor side as: 30°, 60°, 90°, 120° (Tendon 3 direction), and 180°. For each performance, bending action was repeated 10 times for each direction. In this study, bent shape is evaluated by the angle observed from the floor side. Figure 10 shows the examples of the bent shapes in five directions, and target angle is illustrated in green lines.

Experimented results are summarized in Fig. 11, in which the observed bent angles are plotted, together with the corresponding target angles. When manipulated to the 120° direction, the robot was successfully bent to the target direction by pulling the tendon thread #3. In the manipulation to the 60° and 180° directions, the robot was also correctly bent to the target directions by pulling two threads simultaneously with the same speed (threads #1 and #3 for 60° direction, and threads #2 and #3 for 180° direction). When manipulated to the 30° and 90° directions, the angle offset between the target angle and measured angles became greater, compared with other angles. This is because the target directions were situated between two tendons, and the manipulation values were

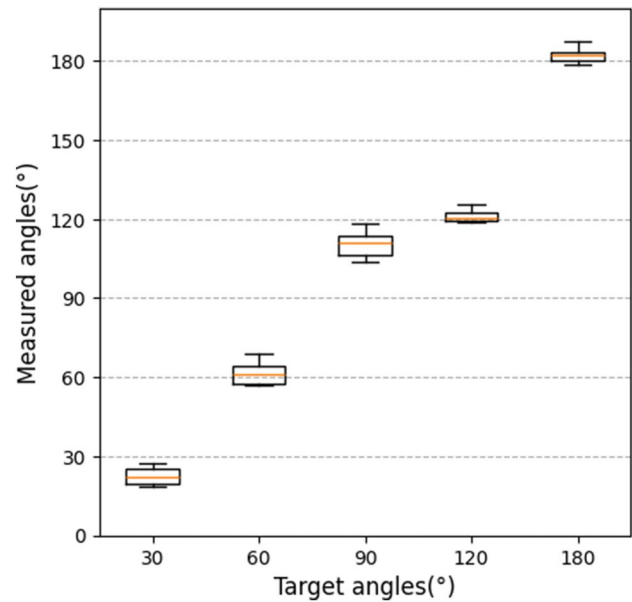


Fig. 11 Measured angles

proportionally given by the interpolation ratio between the two tendons.

Next, we demonstrated to move the tip of the manipulator along an arc. First, the tip was moved about 80 mm to the radial direction of 0° from the initial central

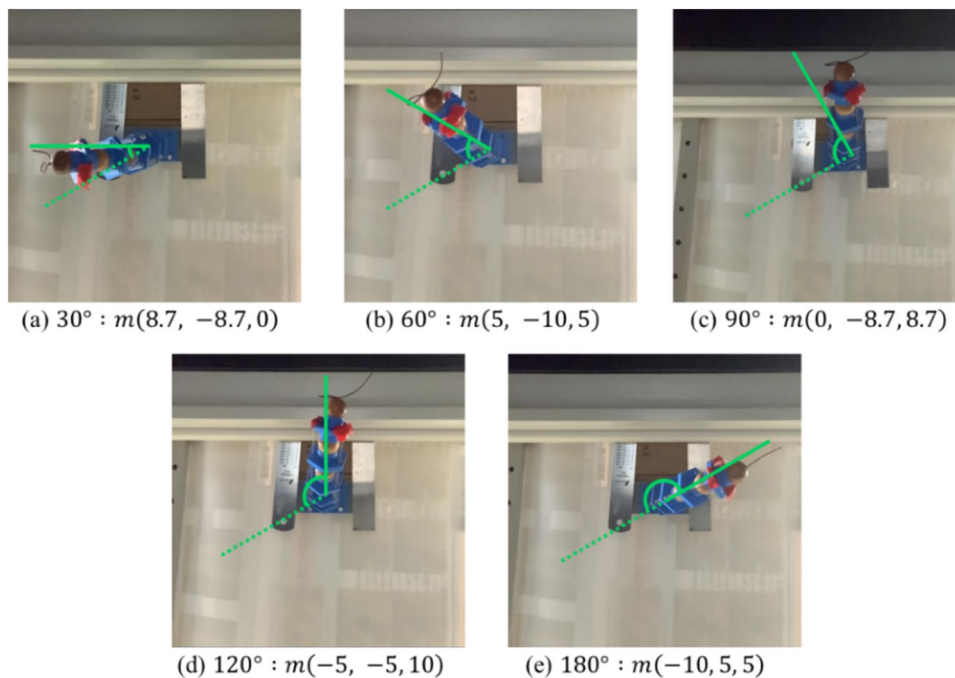


Fig. 10 Manipulation in different angles

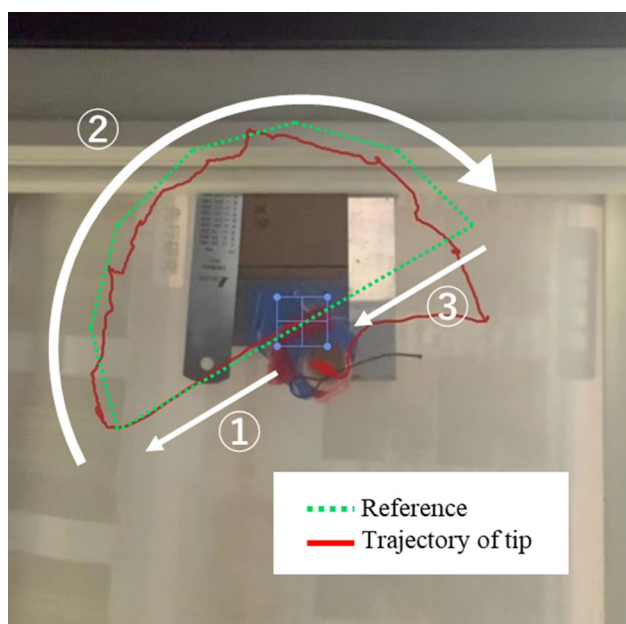


Fig. 12 Trajectory of the tip of the robot

Table 3 Grasped objects

Object	Shape	Size (mm)	Weight (g)
Ball of yarn	Cylinder	ϕ 65	35
Reel	Cylinder	ϕ 33	190
Rubik's cube	Cube	50 × 50 × 50	67
Card case	Rectangular	18 × 65 × 90	100
Cushion	Rectangular	300 × 220 × 80	150

position, and then the angle of the arc was changed from the 20° direction to the 180° direction.

The result of arc-following motion is plotted in red line in Fig. 12, together with the expected trajectory shown in green dotted line. Although there was some misalignment, it was verified that the trajectory operated in accordance with the target trajectory.

Grasping demonstration

To demonstrate the grasping performance of our manipulator, we prepared five objects shown in Table 3. Each object has a different shape and size.

The robot was fixed as shown in Fig. 9. The manipulator grasped these objects by wrapping around them, held them for three seconds, and released them.

As shown in Fig. 13, all the objects were successfully grasped. The numbers in the figures represent the time

taken from the initial state. The manipulator grasped the ball of yarn and the reel, which were shaped like a cylinder, by wrapping around their round bodies (Fig. 13a and b). When the manipulator grasped the Rubik's cube by wrapping, it adjusted its shape to the object's square shape (Fig. 13c). The card case was grasped by pinching it using two points of the manipulator (Fig. 13d). Lastly, the manipulator adjusted to the soft cushion's flexible shape for firm grasping (Fig. 13e). It was confirmed that the objects having different shapes and sizes could be successfully grasped by wrapping around them.

The robot is constructed with the three-fold rotational symmetric structure in the arrangement of tendons. To confirm that the robot can grasp objects in any direction, we experimented with grasping objects by bending it in multiple directions. In the previous grasping experiment, objects were grasped by bending the robot in the direction of 60° presented in Fig. 8. Here, we verified whether the robot could grasp the reel, which was the heaviest object used in the previous experiment, at 0° and 30° bending directions.

Figure 14 shows the grasping results in 0° and 30° directions. The numbers shown in the figures present the time in second taken from the initial state. The robot successfully grasped the reel at all angles, and this experiment confirmed that the robot can generate enough force to grasp objects at any angle.

Discussion

Our manipulator succeeded in grasping objects up to 190 g, which is about 2.4 times the weight of the manipulator itself. This capability is highly dependent on the torque of the used servo motor, so strong motors would make it possible to grasp heavier objects.

Since the manipulator has redundant structure and the robot model (Figs. 7 and 8) is simplified based on several assumptions, it is not suitable for precise control or positional control. Since the design concept of this robot was to combine grasping and omni-directional motion, the experimental results confirmed that these requirements were satisfied.

Conclusions

We designed and constructed a tendon-driven continuum robot manipulator with ball joints to achieve the articulation to arbitrary directions and also to grasp objects with different shapes and weights. The robot is bent by winding the tendons with connected servo motors, and returns to the straightened state by the restoring force of contracted springs settled between the

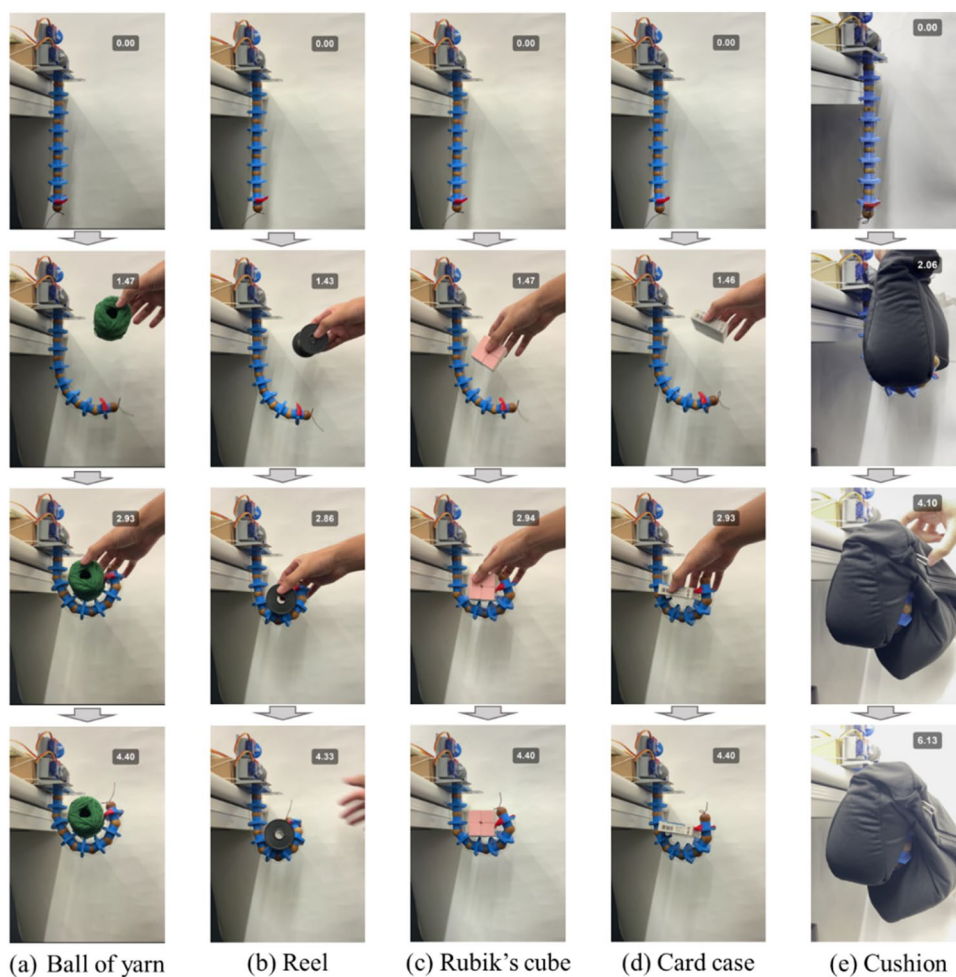


Fig. 13 Grasping experiment

discs. Using this robot, the experiments were conducted to confirm the operability to arbitrary directions and the grasping performance. As a result, the robot successfully moved to arbitrary directions, and also grasped objects having different shapes and sizes.

We will further develop the continuum robot to achieve complex movements that closely resemble those of actual living creatures and grasp various

objects based on these movements. Further complex motions can be realized by making the robot composed of multiple sections. In addition, by introducing machine learning and developing a system that grasps objects in appropriate motion based on visual information, it will be possible to grasp a variety of objects in different environments.

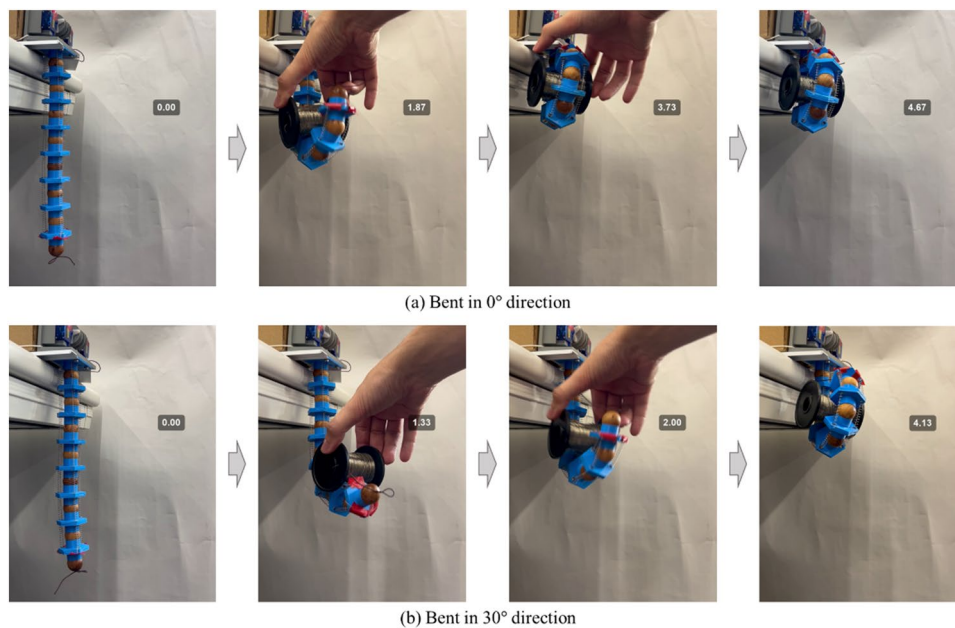


Fig. 14 Grasping performance in different directions

Acknowledgements

Not applicable.

Author contributions

All authors proposed the concept of the robot. RO designed and developed the robot. RO performed the experiments. All authors performed data analysis. All authors read and approved the final manuscript.

Funding

This work is partially supported by JSPS KAKENHI Grant-in-Aid for Scientific Research (B) 20H04214.

Availability of data and materials

All data generated or analyzed during this study are included in this published article.

Declarations

Competing interests

The authors declare that they have no competing interests.

Received: 6 November 2023 Accepted: 14 March 2024

Published online: 26 March 2024

References

- Robinson G, Davies JBC (1999) Continuum robots - a state of the art. In: Proceedings 1999 IEEE International Conference on Robotics and Automation (Cat. No.99CH36288C). 4:2849–2854
- Hannan MW, Walker ID (2001) The “elephant trunk” manipulator, design and implementation. In: 2001 IEEE/ASME International Conference on Advanced Intelligent Mechatronics. Proceedings (Cat. No.01TH8556). 1:14–19
- Liu Y, Ge Z, Yang S, Walker ID, Ju Z (2019) Elephant’s trunk robot: an extremely versatile under-actuated continuum robot driven by a single motor. *J Mech Robot*. <https://doi.org/10.1115/14043923>
- Wang N, Wang D, Zhang Y, Yuan Z, Ge Z, Liu Y (2020) Research on stable envelope holding of elephant-trunk robot driven by single motor. In: 2020 35th Youth Academic Annual Conference of Chinese Association of Automation (YAC). 334–338
- Laschi C, Cianchetti M, Mazzolai B, Margheri L, Follador M, Dario P (2012) Soft robot arm inspired by the octopus. *Adv Robot* 26:709–727. <https://doi.org/10.1163/156855312X626343>
- Walker ID (2013) Continuous backbone “continuum” robot manipulators. *Int Sch Res Not* 2013:e726506. <https://doi.org/10.5402/2013/726506>
- Tsukagoshi H, Kitagawa A, Segawa M (2001) Active Hose: an artificial elephant’s nose with maneuverability for rescue operation. In: Proceedings 2001 ICRA. IEEE International Conference on Robotics and Automation (Cat. No.01CH37164). 3: 2454–2459
- Simaan N, Xu K, Wei W, Kapoor A, Kazanzides P, Taylor R, Flint P (2009) Design and integration of a telerobotic system for minimally invasive surgery of the throat. *Int J Robot Res* 28:1134–1153. <https://doi.org/10.1177/0278364908104278>
- Burgner-Kahrs J, Rucker DC, Choset H (2015) Continuum robots for medical applications: a survey. *IEEE Trans Robot* 31:1261–1280. <https://doi.org/10.1109/TRO.2015.2489500>
- Kang R, Guo Y, Chen L, Branson DT, Dai JS (2017) Design of a pneumatic muscle based continuum robot with embedded tendons. *IEEEASME Trans Mechatron* 22:751–761. <https://doi.org/10.1109/TMECH.2016.2636199>
- Huang X, Zou J, Gu G (2021) Kinematic modeling and control of variable curvature soft continuum robots. *IEEEASME Trans Mechatron* 26:3175–3185. <https://doi.org/10.1109/TMECH.2021.3055339>
- Goergen Y, Chadda R, Britz R, Scholtes D, Koev N, Motzki P, Werthschützky R, Kupnik M, Seelecke S (2019) Shape memory alloys in continuum and soft robotic applications. *Am Soc Mech Eng Digital Collection*
- Sun Y, Liu Y, Lueth TC (2022) Optimization of stress distribution in tendon-driven continuum robots using fish-tail-inspired method. *IEEE Robot Autom Lett* 7:3380–3387. <https://doi.org/10.1109/LRA.2022.3147456>
- Nguyen T-D, Burgner-Kahrs J (2015) A tendon-driven continuum robot with extensible sections. In: 2015 IEEE/RSJ International Conference on Intelligent Robots and Systems (IROS). pp 2130–2135
- Li M, Kang R, Geng S, Guglielmino E (2018) Design and control of a tendon-driven continuum robot. *Trans Inst Meas Control* 40:3263–3272. <https://doi.org/10.1177/0142331216685607>

16. Braganza D, McIntyre ML, Dawson DM, Walker ID (2006) Whole arm grasping control for redundant robot manipulators. In: 2006 American Control Conference. 6
17. Asano F, Luo Z-W, Yamakita M, Hosoe S (2003) Dynamic modeling and control for whole body manipulation. In: Proceedings 2003 IEEE/RSJ International Conference on Intelligent Robots and Systems (IROS 2003) (Cat. No.03CH37453). 3:3162–3167
18. Li L, Jin T, Tian Y, Yang F, Xi F (2019) Design and analysis of a square-shaped continuum robot with better grasping ability. *IEEE Access* 7:57151–57162. <https://doi.org/10.1109/ACCESS.2019.2914124>
19. Li Y, Ren T, Chen Y, Chen MZQ (2020) A variable stiffness soft continuum robot based on pre-charged air, particle jamming, and origami. In: 2020 IEEE International Conference on Robotics and Automation (ICRA). 5869–5875
20. Shah DS, Yang EJ, Yuen MC, Huang EC, Kramer-Bottiglio R (2021) Jamming skins that control system rigidity from the surface. *Adv Funct Mater* 31:2006915. <https://doi.org/10.1002/adfm.202006915>
21. Wei Y, Chen Y, Yang Y, Li Y (2016) A soft robotic spine with tunable stiffness based on integrated ball joint and particle jamming. *Mechatronics* 33:84–92. <https://doi.org/10.1016/j.mechatronics.2015.11.008>
22. Fan Y, Liu D, Ye L (2022) A novel continuum robot with stiffness variation capability using layer jamming: design, modeling, and validation. *IEEE Access* 10:130253–130263. <https://doi.org/10.1109/ACCESS.2022.3228775>
23. Matsuda R, Mavinkurve UK, Kanada A, Honda K, Nakashima Y, Yamamoto M (2022) A woodpecker's tongue-inspired, bendable and extendable robot manipulator with structural stiffness. *IEEE Robot Autom Lett* 7:3334–3341. <https://doi.org/10.1109/LRA.2022.3146954>
24. Yang Y, Chen Y, Li Y, Zhiqiang Chen M (2016) 3D printing of variable stiffness hyper-redundant robotic arm. In: 2016 IEEE International Conference on Robotics and Automation (ICRA). 3871–3877
25. Schmitz A, Treratanakulchai S, Berthet-Rayne P, Yang G-Z (2019) A rolling-tip flexible instrument for minimally invasive surgery. In: 2019 International Conference on Robotics and Automation (ICRA). 379–385
26. Mizuuchi I, Inaba M, Inoue H (2001) A flexible spine human-form robot-development and control of the posture of the spine. In: Proceedings 2001 IEEE/RSJ International Conference on intelligent robots and systems. Expanding the societal role of robotics in the the next millennium (Cat. No.01CH37180). 4:2099–2104
27. Mizuuchi I, Yoshida S, Inaba M, Inoue H (2003) The development and control of a flexible-spine for a human-form robot. *Adv Robot* 17:179–196. <https://doi.org/10.1163/156855303321165123>

Publisher's Note

Springer Nature remains neutral with regard to jurisdictional claims in published maps and institutional affiliations.